

# Microwave Intermodulation Technique for Monitoring the Mechanical Stress in RF MEMS Capacitive Switches

Cristiano Palego<sup>1</sup>, Subrata Hadler<sup>1</sup>, Bora Baloglu<sup>1</sup>, Zhen Peng<sup>1</sup>, James C. M. Hwang<sup>1</sup>, Herman F. Nied<sup>1</sup>, David I. Forehand<sup>2</sup>, and Charles L. Goldsmith<sup>2</sup>

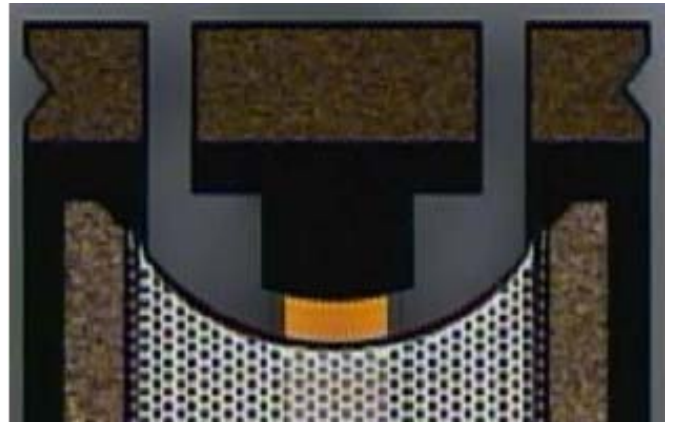
<sup>1</sup>Lehigh University, Bethlehem, PA 18015, USA. <sup>2</sup>MEMtronics Corp., Plano, TX 75075, USA.

**Abstract** — For the first time, a microwave intermodulation technique is used to measure the mechanical resonance directly on packaged and unpackaged RF MEMS capacitive switches with quality factors approaching unity due to air damping. The result is validated by similar measurements in vacuum with much higher quality factors. From the measured resonance frequencies, the residual mechanical stress of the fixed-fixed membrane of the switches is derived and its temperature dependence is analyzed and correlated with that of the pull-in voltage. The present technique offers a convenient means for monitoring the residual stress in RF MEMS devices in both manufacturing and operation. It also allows mechanical and electrical degradation effects to be conveniently separated during life testing of the switches.

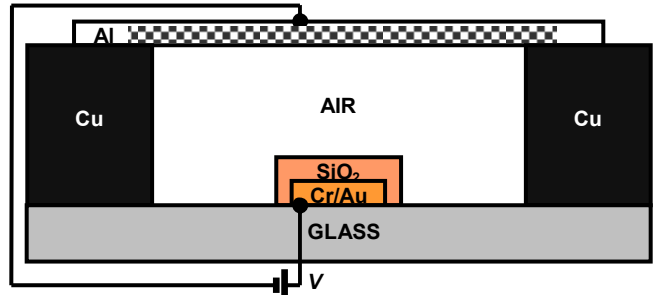
**Index Terms** — Intermodulation distortion, microelectromechanical devices, microwave devices, microwave measurements, microwave switches, resonance, stress, stress control, stress measurement, switches.

## I. INTRODUCTION

Recently, significant progress has been made in improving the robustness of RF MEMS capacitive switches through dielectric-charging mitigation [1], device-level packaging [2], and power-handling enhancement [3]. To ensure robust operation of these switches in harsh environments, such as elevated temperatures, the residual mechanical stresses in the fixed-fixed membrane of the switches, packaged or unpackaged, must be carefully monitored and controlled in both manufacturing and operation. This is because the stress increases not only the restoring force of the membrane (preventing stiction), but also the pull-in voltage  $V_p$  of the membrane (aggravating dielectric charging). The stress of the membrane can be inferred from its mechanical resonance frequency, which is typically on the order of 100 KHz. However, there is no easy way to measure the resonance on the switches directly, especially in packaged form. This is because, for minimum insertion loss, shunt switches are designed to have small ( $\leq 100$  fF) off-state (with the membrane suspended) capacitance, so that any variation of the capacitance due to mechanical vibration is correspondingly small. In addition, for quick return to the off state without ringing, significant air damping is relied upon to keep the quality factor low. To overcome these challenges, we use a microwave intermodulation technique to detect small capacitance variations as described in the following.



(a)



(b)

Fig. 1. (a) Top and (b) cross-section views of an RF MEMS capacitive switch. In (a), only the upper half of the switch is shown; the lower half is a mirror image of the upper half. In (b), the vertical scale is expanded by approximately 60X for clarity.

Fig. 1 illustrates the switch used in the present experiment [4]. The bowtie-shaped aluminum membrane has a thickness  $t = 0.3 \mu\text{m}$ , length  $L = 310 \mu\text{m}$ , and width  $W = 120\text{-}250 \mu\text{m}$ . The membrane is perforated with a honeycomb pattern of holes. The hole diameter is  $7 \mu\text{m}$  and the center-to-center spacing of the holes is  $12 \mu\text{m}$ , unless otherwise noted. The perforation is mainly for removal of sacrificial photoresist rather than adjustment of air damping or residual stress.

The behavior of four switches is measured. Switch 1 and Switch 2 have exactly the same design as described above. Switch 3 is perforated with  $8\text{-}\mu\text{m}$  holes, with a spacing of 11

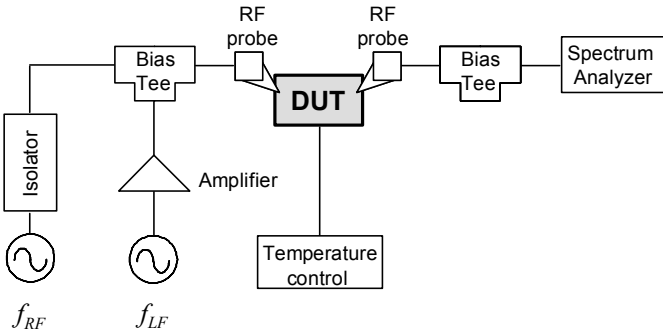


Fig. 2. Microwave intermodulation measurement setup.

μm. Switches 1, 2 and 3 are fabricated on the same wafer and are unpackaged. Switch 4 is of the same design as Switches 1 and 2, but fabricated on a different wafer and is packaged [2]. Based on the measured off-state capacitance, the air gap  $g = 2.2 \mu\text{m}$  for Switches 1, 2 and 3, while  $g = 2.6 \mu\text{m}$  for Switch 4. Larger air gap corresponds to higher pull-in voltage so that, at room temperature,  $V_p = 34 \text{ V}$  for Switch 4 while  $V_p = 25 \text{ V}$  for Switches 1, 2 and 3.

## II. MEASUREMENT TECHNIQUE

Fig. 2 illustrates the microwave intermodulation measurement setup. The input of the switch comprises a 0-dBm microwave ( $f_{RF} = 10 \text{ GHz}$ ) signal and a low-frequency ( $f_{LF}$ ) signal that is swept from 10 to 150 KHz with an amplitude of approximately 10 V. The microwave and low-frequency signals are mixed through the squared voltage dependence of the electrostatic force exerted on the membrane, with its mechanical response acting as a low-pass filter. Fig. 3 shows that this results in dominant sideband components of  $f_{RF} \pm 2f_{LF}$  on the output spectrum [5], [6]. Fig. 4 plots the relative magnitudes of these sideband components measured on Switch 1 as a function of  $f_{LF}$  and ambient temperature  $T$ , the ambient being air with less than 1% humidity. The resonance frequency is more prominent on a linear, as opposed to logarithmic, scale and it decreases from 208 to 83 KHz as the temperature is increased from 25 to 75°C.

To assess the air-damping effect, the measurement is repeated at 30°C in both air and vacuum. Fig. 5 shows that the resonance is much sharper in vacuum but the peak frequency shifts by only 8%. This shift in resonance frequency can be used to extract the mechanical quality factor according to a simple 2<sup>nd</sup> order model:

$$f_N = \sqrt{1 - 1/4Q^2} \cdot f_{N0}, \quad (1)$$

where  $f_N$  and  $f_{N0}$  are the damped and undamped resonance frequencies, respectively, and  $Q$  is the quality factor. The resulting  $Q=1.2$  is close to unity by design.

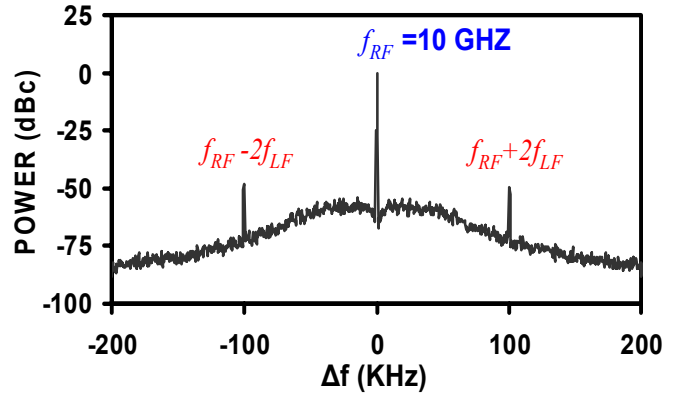


Fig. 3. Output spectrum of Switch 1 in dry air and ambient temperature showing carrier and sideband components under an input power of 0 dBm.

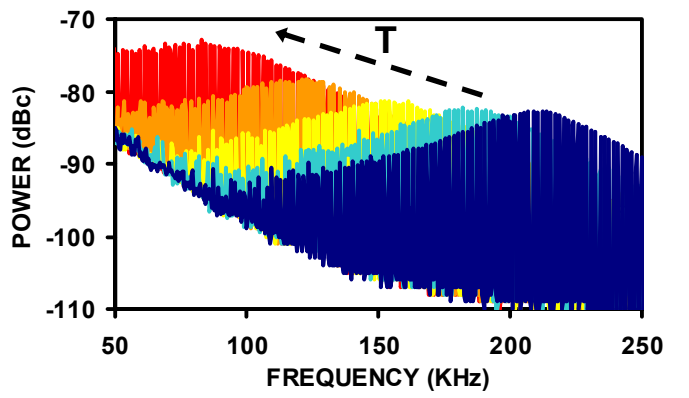


Fig. 4. Relative magnitudes of  $f_{RF} \pm 2f_{LF}$  sideband components measured on the output spectrum of Switch 1 as a function of  $f_{LF}$  and  $T$ , with  $T = 25, 0, 25, 50$  and  $75^\circ\text{C}$  right to left.

## III. MECHANICAL MODEL

For a fixed-fixed rectangular aluminum beam subjected to a uniform uniaxial stress  $\sigma$  in vacuum, the resonance frequency is [7], [8]:

$$f_{N0} = \frac{t}{L^2} \cdot \sqrt{\frac{E}{\rho}} \cdot \sqrt{1 + \frac{3\sigma(1-\nu)L^2}{E\pi^2 t^2}}, \quad (2)$$

where the Young's modulus  $E = 70 \text{ GPa}$ , the density  $\rho = 2.7 \text{ g/cm}^3$ , and Poisson's ratio  $\nu = 0.35$ . Because the actual geometry is rather complicated, finite-element analysis is used to determine the mechanical properties of an equivalent rectangular beam that has the same moment of inertia as that of the perforated and bowtie-shaped membrane. Thus, for the equivalent rectangular beam in air  $W' = 180 \mu\text{m}$ ,  $E' = 0.5E$ ,  $\rho' = 0.68\rho$ ,  $\nu' = 0.6$ , and

$$f'_N = \sqrt{1 - \frac{1}{4Q^2}} \cdot \frac{\beta t}{L^2} \cdot \sqrt{\frac{E'}{\rho'}} \cdot \sqrt{1 + \frac{3\sigma(1-\nu')L^2}{E'\pi^2 t^2}}, \quad (3)$$

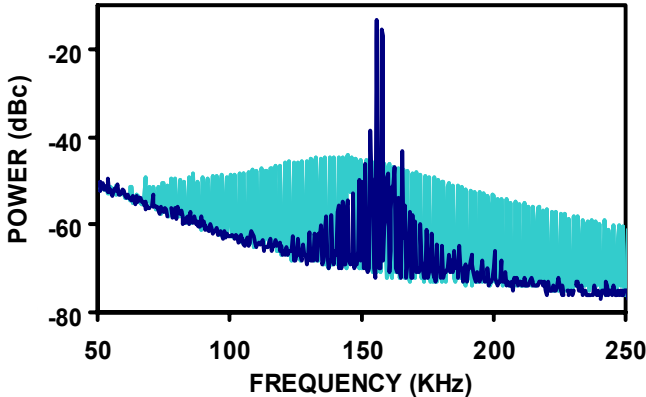


Fig. 5. Relative magnitudes of  $f_{RF} \pm 2f_{LF}$  sideband components measured on the output spectrum of Switch 1 in (lighter curves) air and (darker curves) vacuum.

where air damping is modeled as in (1) with the temperature and frequency dependence of  $Q$  neglected, and  $\gamma$  is a geometrical factor that captures the difference in mechanical behaviors other than the moment of inertia. Empirically,  $\gamma = 0.6$  for the present switches. Usually,  $3\sigma(1-\nu')L^2 \gg E' t^2$  and  $f_N \propto \sqrt{\sigma}$ .

Similarly, the pull-in voltage is proportional to  $\sqrt{\sigma}$  according to the following [4]:

$$V_p = \sqrt{\frac{64\gamma\sigma(1-\nu')tg^3}{27L^2\varepsilon}}, \quad (4)$$

where  $\gamma$  is another geometrical factor similar to  $\gamma$  ( $\gamma = 1.1$  for the present switches), and  $\varepsilon$  is the permittivity of air. Eq. (4) assumes a pristine membrane that has never been pulled down by applying a voltage higher than  $V_p$ . If the switch has been repeatedly operated, then charge  $Q$  may accumulate in the dielectric and (4) needs to be modified to include the dielectric-charging effect [1]:

$$V'_p = \sqrt{\frac{64\gamma\sigma(1-\nu')tg^3}{27L^2\varepsilon}} - \frac{hQ}{\varepsilon}, \quad (5)$$

where  $Q$  is assumed to be a sheet charge at a height of  $h$  above the bottom electrode.

#### IV. RESULTS AND DISCUSSION

To validate the above approach, the resonance frequency measurement is performed on unpackaged Switches 1, 2 and 3 as well as the packaged Switch 4. Fig. 6 shows the consistent results among the four switches. This implies that the slightly different perforation pattern of Switch 3 is not sufficient to make it behave significantly differently from Switches 1 and 2, while the packaging process of Switch 4 does not affect its mechanical behavior either.

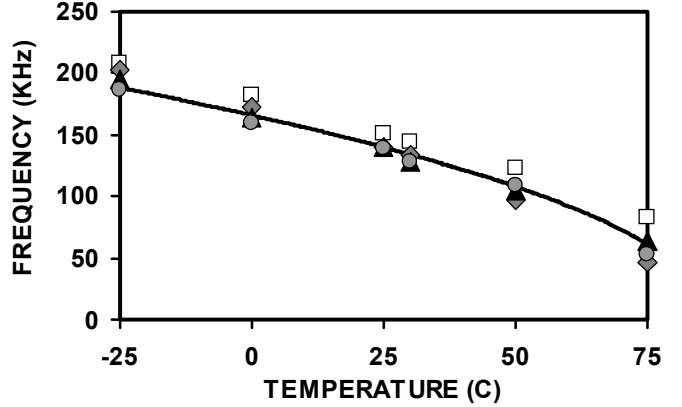


Fig. 6. (symbols) Measured vs. (curve) modeled resonance frequencies in air as a function of temperature for unpackaged Switches (□) 1, (Δ) 2, and (◆) 3 and packaged Switch (●) 4.

Fig. 7 shows that the residual stress extracted according to (3) from the measured resonance frequencies is on the order of 100 MPa, and decreases linearly with temperature:

$$\sigma(T) = \Delta\alpha E'(T_0 - T), \quad (6)$$

where  $\Delta\alpha = 20 \text{ ppm}/^\circ\text{C}$  is the difference in the thermal expansion coefficients of the aluminum membrane and the glass substrate, and  $T_0 = 86^\circ\text{C}$  for the present switches.

By inserting (6) into (4), Fig. 8 shows that the modeled pull-in voltage agrees with that measured, and the higher pull-in voltage of Switch 4 can be explained by its larger air gap. Conversely, if the air gap is precisely known, the pull-in voltage can also be used to gauge the residual stress. However, unlike the resonance measurement, measurement of the pull-in voltage involves actuation of the switch and possible electrical degradation effects such as dielectric charging. In this case, mechanical and electrical degradation effects may occur simultaneously and (5) instead of (4) needs to be used.

Due to the uncertainties in air-damping ( $Q$ ), mechanical ( $E'$  and  $\nu'$ ), and geometrical ( $\beta$ ) parameters, there is significant uncertainty in the absolute value of the extracted residual stress. For example, (1) implies that for the present switches, if air damping is not considered, the absolute stress extracted by using (3) will have a 17% error. However, this should not prevent the present technique from being used to monitor the relative change in the residual stress from device to device, from wafer to wafer, and under different manufacturing processes and operating conditions.

Actually, the stress distribution in the membrane is not likely to be uniform or uniaxial as assumed in (2)-(5) and alternative techniques may be used to determine the precise stress at different locations on the membrane. Again, this should not distract from the value of an average or effective stress parameter, which can be conveniently monitored and compared for fixed switch geometries.

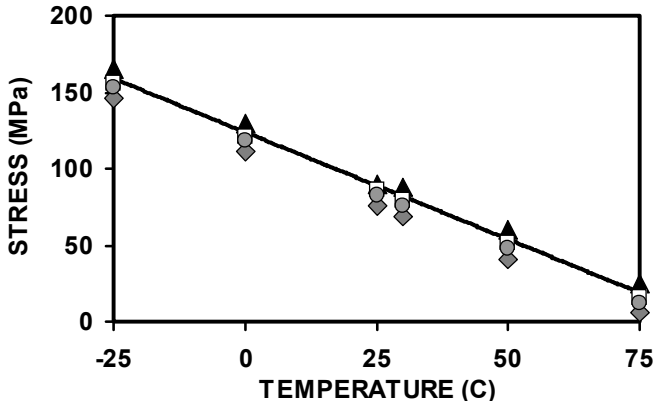


Fig. 7. (symbols) Measured vs. (curve) modeled residual stresses as a function of temperature for unpackaged Switches (□) 1, (Δ) 2, and (◆) 3 and packaged Switch (●) 4.

Eqs. (2) and (3) are valid only for linear mechanical response with small deflections. The assumption appears to be valid due to the high aspect ratio of >100:1 for the membrane length over the air gap. Furthermore, the deflection of interest is limited to one third of the air gap, beyond which the membrane snaps down and the capacitance increases abruptly. Experimentally, an LF signal of  $0.4V_p$  in vacuum or  $0.6V_p$  in air is sufficient to produce detectable sideband components at the output. On the other hand, the resonance frequency of  $f_{RF} \pm 2f_{LF}$  shifts less than a few KHz, even when the low-frequency signal is increased to  $0.95V_p$  and other sideband components are produced. This underscores the robustness of the present technique.

The present experiment is limited to 75°C or lower. Above 75°C, the membrane sags, the quality factor drops below unity, and  $f_{RF}$  approaches the range of the phase noise of the RF generator. Better understanding of these phenomena can help extend the temperature range of the switches.

## V. CONCLUSION

A microwave intermodulation technique is developed for the measurement of mechanical resonance frequency and residual stress for fixed-fixed beams with and without air damping. This technique has been applied to packaged and unpackaged RF MEMS capacitive switches without special test structure or vacuum. The measured square-root temperature dependence of both the resonance frequency and the pull-in voltage is consistent with a residual stress that decreases linearly with temperature. Since the pull-in voltage can be affected by other factors such as dielectric charging, the present technique provides an effective and convenient means to separate the mechanical effects from electrical effects in long-term life tests as illustrated in (5).

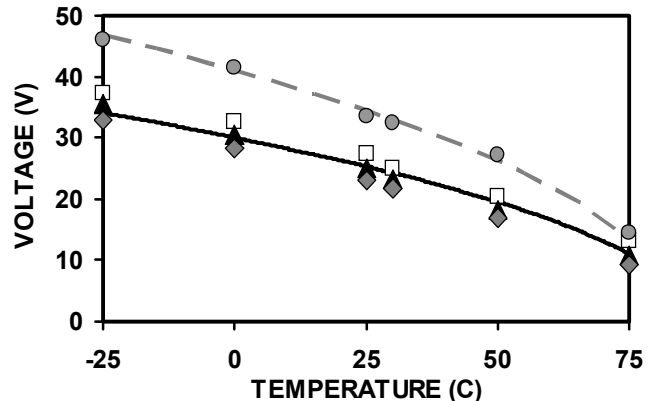


Fig. 8. (symbols) Measured vs. (curves) modeled pull-in voltages as a function of temperature for unpackaged Switches (□) 1, (Δ) 2, and (◆) 3 and packaged Switch (●) 4.

## ACKNOWLEDGEMENT

The authors wish to acknowledge IBM for making the vacuum probe station available with the technical assistance of C. V. Jahnes and J. Cotte. This work is supported in part by the US Defense Advanced Research Projects Agency under the Harsh Environment, Robust Micromechanical Technology (HERMIT) Program (Contract No. F33615-03-C-7003) and the N/MEMS Science & Technology Fundamentals Research Program (Grant No. HR0011-06-1-0046), as well as the Commonwealth of Pennsylvania, Department of Community and Economic Development through the Pennsylvania Infrastructure Technology Alliance (PITA).

## REFERENCES

- [1] C. L. Goldsmith, D. I. Forehand, Z. Peng, J. C. M. Hwang, and J. L. Ebel, "High-cycle life testing of RF-MEMS switches," *IEEE MTT-S Int. Microwave Symp Dig.*, pp. 1805-1808, June 2007.
- [2] D. I. Forehand, and C. L. Goldsmith, "Wafer level micropackaging for RF-MEMS switches," *ASME InterPACK Tech. Conf. Dig.*, July 2005.
- [3] C. Palego, A. Pothier, T. Gasseling, A. Crunceanu, C. Cibert, C. Champeaux, P. Tristant, A. Catherinot, and P. Blondy, "RF-MEMS switched varactor for high power applications," *IEEE MTT-S Int. Microwave Symp Dig.*, pp. 35-38, June 2006.
- [4] C. L. Goldsmith, and D. I. Forehand, "Temperature variation of actuation voltage in capacitive MEMS switches," *IEEE Wireless Components Lett.*, vol. 15, pp. 718-720, Oct. 2005.
- [5] D. Mercier, P. Blondy, D. Cross, and P. Guillon, "An electromechanical model for MEMS switches," *IEEE MTT-S Int. Microwave Symp Dig.*, pp. 2123-2126, May 2001.
- [6] L. Dussopt, and G. M. Rebeiz, "Intermodulation distortion and power handling in RF MEMS switches, varactors, and tunable filters," *IEEE Trans. Microwave Theory Techniques*, vol. 51, pp. 1247-1255, April 2003.
- [7] S. S. Rao, *Mechanical Vibrations*, Reading: Addison Wesley, 1986.
- [8] P. M. Osterberg, and S. D. Senturia, "M-TEST: a test chip for MEMS material property measurement using electrostatically actuated test structures," *IEEE J. Microelectromechanical Systems.*, vol. 6, pp. 107-118, June 1997.